Journal of Food Engineering 387 (2025) 112353

Contents lists available at ScienceDirect

Journal of Food Engineering

journal homepage: www.elsevier.com/locate/jfoodeng

Effects of oil-water interfacial properties on protein structuring and droplet deformation in high moisture meat analogues containing oil

Naoya Ikenaga [a,b,c], Shuzo Hashimoto [a,b], Leonard M.C. Sagis [a,*]

[a] Laboratory of Physics and Physical Chemistry of Foods, Wageningen University & Research, Bornse Weilanden 9, 6708 WG, Wageningen, the Netherlands
[b] Fuji Oil Global Innovation Center Europe, Bronland 10, 6708 WH, Wageningen, the Netherlands
[c] Fuji Oil Co., Ltd., 1 Sumiyoshi-cho, Izumisano-shi, Osaka, 598-8540, Japan

ARTICLE INFO

Keywords:
Potato protein
Pea protein
Emulsion stability
Extrusion
Meat analogue
Oil droplet deformation

ABSTRACT

Adding oil to high moisture meat analogues (HMMA) can increase juiciness, and can be achieved by incorporating emulsion droplets during extrusion. Since these droplets can coalesce when subjected to high shear, selecting appropriate emulsion stabilisers is important. For several commercial plant-protein emulsion stabilisers, it was investigated how oil-water interfacial mechanical properties affect droplet deformation and protein structuring in extrusion of HMMAs. Emulsions with 10 wt% or 15 wt% oil, stabilised by potato protein isolates (POPI-1 (Rich in patatin) and POPI-2 (rich in protease inhibitor)) and pea protein isolate PPI, were used to make extrudates with 5.7 wt% and 8.5 wt% oil, respectively. In 8.5 wt%-extrudates, POPI-2 had the most oil leakage from the cooling die, while PPI had the smallest amount despite having softer and more stretchable interfaces. Blade-cutting tests showed the highest maximum force for 8.5 wt%-extrudates with POPI-1, likely because POPI-1 formed the stiffest interfaces. Tensile stress testing showed the largest fracture strain in 8.5% wt%-extrudates with PPI, corresponding to its longer wedge length. Multiphoton excitation microscopy was used to visualise the extrudates protein structure and oil droplets. This showed that droplets near the surface of the extrudate were less deformed than droplets in the centre. There were only small differences between protein stabilisers regarding oil droplet deformation, indicating droplet deformation was dominated by deformation of the protein matrix. The O/W interfacial properties significantly affected oil leakage, cutting force, and tensile strength of extrudates. These results are important to consider when designing emulsions for HMMAs processed by extruders.

1. Introduction

Sustainability aspects have become important for food product development, and one option to improve the sustainability of food products is replacing dairy- and meat-based proteins with plant-based proteins (Akharume et al., 2021; Cornet et al., 2022; Mäkinen et al., 2016; Mefleh et al., 2022; Munekata et al., 2020; Singh et al., 2021). An example is the production of plant-based meat analogues. They are often produced by high moisture extrusion in an attempt to mimic the fibrous structure of meat (Pietsch et al., 2017; Pietsch et al., 2019), and are then referred to as high moisture meat analogues (HMMA). To obtain tasty and juicy HMMAs, flavours and moisture need to be retained during the extrusion process (Guo et al., 2020). Oils and fats are important for juiciness in animal meat (Choi et al., 2019), and the lack of them can be a problem for the taste and juiciness of plant-based meat analogues. Possible ways to add them to plant-based meat analogues are to mix bulk oil and fat directly into the feed of an extruder or mix them in the form of small emulsion droplets. Recently, these two methods were compared (Gwiazda et al., 1987; Kendler et al., 2021). The direct addition of oil affected essential parameters to texturise proteins and caused reductions in temperature and die pressure (Osen et al., 2014; Zhang et al., 2020). These parameter changes make adding enough oil to HMMAs to achieve animal meat-like juiciness very difficult. An emulsion with 8 wt% oil content improved protein texturising compared to direct oil addition (Wang et al., 2022). However, the fibre length of the proteins was still insufficient to imitate animal meat in terms of texture.

In addition, in high moisture extrusion, emulsion droplets are exposed to high deformation rates, which can lead to disruption of the microstructure of the interfacial film stabilising the droplet, resulting in coalescence (Emin and Schuchmann, 2013). As a result, oil can accumulate at the wall of the extruder, reducing the friction between the wall and the protein material and leading to flow instabilities, oil leakage,

* Corresponding author.
E-mail address: leonard.sagis@wur.nl (L.M.C. Sagis).

https://doi.org/10.1016/j.jfoodeng.2024.112353
Received 2 August 2024; Received in revised form 7 October 2024; Accepted 10 October 2024
Available online 11 October 2024

and heterogeneities in the product. Clearly, to produce meat-like structures containing emulsion droplets, the stability of the incorporated emulsion droplets at high strain (rate) is an essential design parameter.

The emulsions incorporated in meat replacers are typically stabilised by proteins, either the same one used for the bulk of the product or a different one, specifically added to stabilise the emulsion. Proteins are known to form charged and stiff viscoelastic solid-like films after adsorption at the oil-water interface, providing stability against coalescence by imparting mechanical stiffness to the interface and electrostatic repulsion. A general assumption is that a stiffer protein film will result in higher stability against coalescence. However, recent results have shown that such stiff protein films can show yielding when a critical strain is exceeded, resulting in significant softening of the interfacial structure (Sagis and Yang, 2022). As a result, an emulsion that is stable under quiescent conditions may become unstable under the high strain (rate) conditions encountered in an extruder. However, the dynamic behaviour of interfaces at large strains or shear rates, such as those encountered in the food manufacturing process, has not been extensively studied. For an efficient design of juicy plant-based HMMAs containing emulsion droplets, it is important to establish the relationship between the interfacial properties of the emulsion used in extrusion and the final structure and stiffness of the HMMA.

This study explores how interfacial properties of the O/W interface affect the protein structuring and oil droplet deformation in the extrusion process for plant-based HMMAs. First, the extrudates were prototyped using emulsions with 10 wt% and 15 wt% oil content, stabilised by potato and pea proteins. Those proteins were chosen because after adsorption, they form viscoelastic solid structures at the oil-water interface with a wide range in interfacial stiffness, and stretchability, to determine how these parameters affect the protein structuring in extrusion. During extrusion, surface oil on the extrudates and oil leakage from the cooling die outlet were measured. The extrudates were also analysed concerning rheological properties like cutting force and tensile strength using a texture analyser. The wedge length and angle were also measured. The protein structure and oil droplets were observed using multiphoton excitation microscopy, and the droplets were analysed using image analysis in terms of deformation and shape. The results obtained here can facilitate the development of novel juicy meat replacers.

2. Materials and methods

2.1. Materials

Medium-chain triglyceride (MCT) oil (MIGLYOL® 812N) was purchased from IOI Oleochemical (France). Commercial potato protein isolates (POPI), Solanic® 200 (POPI-1) and Solanic® 300 (POPI-2) were kindly donated by Avebe U.A. (Netherlands). A commercial pea protein isolate, Nutralys F85F (PPI), was purchased from Roquette Frères (France). A commercial soy protein concentrate (SPC), ALPHA® 8, was purchased from Solae Europe S.A. (Switzerland). Details of the protein isolates on protein content and weight average molecular weight are given in Table 1. Milli-Q water (PURELAB® Ultra Water Purification System, Germany) was used for emulsion preparation and analyses. Hydrochloric acid (HCl), sodium hydroxide (NaOH), sodium chloride (NaCl), 99.5 v/v% ethanol, and Rhodamine B were purchased from Merck (Germany). BODIPY 505/515 was purchased from Thermo Fisher Scientific (Netherlands).

2.2. Methods

2.2.1. Sample preparation

2.2.1.1. Protein solutions. The protein content of all protein powders was determined beforehand by the Dumas method (conversion factor: 5.5). Based on Dumas results, all powders were dissolved in Milli-Q water at a concentration slightly higher than 1.76 wt%. The solutions were stirred at 20 °C for 4 h, then at 4 °C for 20 h. The pH and conductivity of the solutions were adjusted using 1.0 M HCl, 1.0 M NaOH, and NaCl to pH 3.6 (only for POPI-2)/pH 7.0 (for the others) and 1500 μS/cm. After that, the protein content was adjusted to 1.76 wt%, and the emulsions were stored at 4 °C until used.

2.2.1.2. Emulsion preparation. Emulsions with 10 wt% or 15 wt% MCT oil content were prepared with the protein solutions. The mixtures were first pre-homogenised using an L5M-A Silverson laboratory mixer with a 1 mm screen hole (Silverson Machines Ltd., United Kingdom) at 5000 rpm for 5 min. Then, the pre-homogenised mixture was homogenised by a GEA Lab Homogenizer PandaPLUS 2000 (GEA Group AG, Germany). The beaker for the pre-homogenisation and the homogenisation were in ice water during (pre-)homogenisation to prevent excessive heating. The pressure and the number of passes for the homogenisation are shown in Table 2. The emulsions were collected in a blue cap bottle and stored overnight at 4 °C before analysis. The particle size distribution was measured, confirming that it had a main peak at 0.9–1.0 μm (data not shown).

2.2.1.3. Extrusion experiments. The extrusion experiments were performed using a co-rotating twin-screw extruder, TwinLab-F 20/40 (Brabender GmbH, Germany), with an L/D ratio of 40 and a screw diameter of 20 mm, as described by Nieuwland, Heijnis, van der Goot, and Hamoen (2023). Three 100 mm blocks with a 25 × 7 mm geometry were continuously attached as a cooling die after the main barrel of the extruder. The same screw was used as described by Nieuwland et al. (2023). SPC was dosed via a Brabender Screw Feeder DDSR20 (Brabender GmbH, Germany) at the inlet located at 0D. The water/emulsion was dosed via a peristaltic pump, Watson-Marlow 120U (Watson-Marlow Limited, UK), at the inlet located at 10D. Emulsions were gently remixed before dosing to the extruder, to counteract any creaming

Table 2
Conditions of the homogenisation for emulsions stabilised by potato protein (POPI-1 and POPI-2) or pea protein (PPI). The conditions were adjusted to get similar particle sizing results for all proteins.

Emulsifier	Oil content of emulsion (wt %)	Pressure (bar)	The number of passes
POPI-1	10	130	6
	15	150	6
POPI-2	10	110	6
	15	110	6
PPI	10	110	6
	15	110	8

Table 1
Details of the protein isolates for potato protein (POPI-1 and POPI-2) and pea protein (PPI). Protein content was measured by the Dumas method (see Sec 2.2.1.1), and weight average molecular weight was obtained using HPLC.

Supplier	Source	Protein name	Processing by supplier	pH	Protein content (wt%)	Weight average molecular weight (kDa)
Avebe	Potato	POPI-1	Extracted from potato protein	Neutral	77.18	80
		POPI-2	Extracted from potato protein	Acidic	77.67	32
Roquette	Pea	PPI		Neutral	69.36	94

during storage. The same constant extrusion settings, as described by Nieuwland et al. (2023), were applied for all experiments in this study. The extrudates were cut on a roller band and used for all analyses. All formulations for the extrudate with/without emulsions are shown in Table 3.

2.2.1.4. Surface oil. The extrudate weight of about 8 cm was measured with an aluminium cup. Then, the extrudate surface, except for the two cutting surfaces, was washed with 99.5 v/v% ethanol, and the liquid was collected in the same aluminium cup. The aluminium cup was dried in an oven at 40 °C overnight, and the remaining oil in the cup was weighed. The percentage of surface oil was calculated by dividing by the amount of oil initially added:

$$\text{Surface oil } (wt\%) = \frac{\text{Oil in cup } (g) \times 100\%}{\text{Oil from emulsion } (g)} \quad (1)$$

2.2.1.5. Oil leakage. The oil drops from the outlet of the cooling die during the extrusion experiments were collected in a plastic cup for approximately 10 min. The cups with leaked oil were dried in an oven at 40 °C overnight, and the remaining oil in the cup was measured. The rate of oil leakage was calculated using

$$\text{Rate of oil leakage } (g/h) = \frac{\text{Oil in cup } (g) \times 3600\ (s)}{\text{Time for oil collecting } (s)}. \quad (2)$$

2.2.1.6. Blade cutting. The cutting force was measured, as described by Osen et al. (2014), with small modifications, at room temperature in the direction transverse to the direction of flow, F_t, and longitudinal direction, F_l (Fig. 3), using a texture analyser TA. TX plus with a blade (Warner Bratzler) (Stable Micro Systems Ltd, United Kingdom). The extrudate was cut into a piece 20 mm long and 25 mm wide (Fig. 3). The maximum force during a strain sweep of 0–80% with a test speed of 1 mm/s was recorded in both directions, as $F_{t,max}$ and $F_{l,max}$ for each, using a trigger force of 0.5 N.

2.2.1.7. Tensile stress. The tensile stress was measured as described by Köllmann, Schreuders, Zhang, and van der Goot (2023) with small modifications. The measurements were performed at room temperature with a texture analyser TA. TX plus (Stable Micro Systems Ltd, United Kingdom) using a trigger force of 0.05 N. A uniaxial tensile test was performed with a test speed of 2 mm/s. The extrudate was cut into a dog bone shape, as shown in Fig. 4C. A laser blade cutter was used to cut the samples into a dog bone shape, rather than a mould, since the latter caused too much damage to the protein structure, and the edges could not be made as sharp compared to a laser blade. The measured tensile force at fracture (F_{max} (N)) was used to calculate the tensile strength (σ_{max} (kPa)) with

$$\sigma_{max} = \frac{F_{max} \times 10^{-3}}{A}, \quad (3)$$

where A (m^2) is the cross-section area (width of 15 mm and thickness of 7 mm). The strain was calculated using

$$\gamma = \frac{L(t) - L(0)}{L(0)}. \quad (4)$$

Here, $L(t)$ is the sample length at time t, and $L(0)$ is the sample length at the start of the measurement. The Young's modulus (kPa) was calculated from the slope of the stress-strain curve between $\gamma = 0.05$ and 0.10.

2.2.1.8. Wedge length and angle. The wedge length and angle of the extrudates were measured using the image processing software ImageJ (National Institutes of, USA). The extrudates were split down the middle by tearing along the sample flow direction, and pictures of the wedge were taken (Fig. 4C and D). For the wedge length, a line was drawn connecting each end point of the wedge (the dashed line in Fig. 4C). The distance from the midpoint of that line to the apex was measured (Fig. 4C). The wedge length was then taken as the average of the wedge length for the six wedge shapes each from two replicated extrusion experiments (n = 12 in total). For the wedge angle, the sample images were divided into six slices, and the angle was determined from the 2nd and 5th slices. Two lines were drawn, one along the sample flow direction on the boundary line and the other through the points where the wedge lines intersect the boundary lines of the slices (Fig. 5D). The angle was then taken as the average of six angle values on the 2nd and 5th slices each, from two replicated extrusion experiments (n = 24 in total).

2.2.1.9. Multiphoton excitation microscopy. The samples were cut in the middle in the flow direction, and their cross-sections were dyed (Fig. S1). The dye solution was a mixture of 0.25 mg/mL BODIPY 505/515 solution and 0.04 mg/mL Rhodamine B solution in a 1:1 ratio. The cut samples were put on 30 μL of the dye solution in a dark place for 15 min at 5 °C. Then, the dyed surface was carefully washed twice with Milli-Q water and observed using a multiphoton excitation microscope Leica SP8Dive (Leica, Germany) with an HC PL IRAPO 40x/1.10 Water objective. The laser excitation wavelength was set at 1000 nm (with power at 1.2%), and the emission ranges for BODIPY 505/515 and Rhodamine B were 500–550 nm and 590–650 nm, respectively (with the gain set at 20% for both). The cross-section was divided into 30 fields of view (FOV), and observations were performed at the 3rd, 6th, and 9th FOV, counted from the top (Fig. S1). At each position, 3-dimensional images of the visible fluorescence area were obtained by the z-stack function (Multiphoton mode).

2.2.1.10. Image analysis. From each 3-dimensional image, a slice of about 10 μm thickness (17 images from z-stack), starting from 5 μm below the surface of the 3-dimensional image, was converted to grey-scale using the software LAS X (Leica, Germany). All 17 images from the oil observation channel (500–550 nm for BODIPY 505/515) were analysed using the image processing software ImageJ. The 17 images were summed into one image and analysed using the Area, Perimeter, and Fit ellipse functions to obtain droplet area, perimeter and orientation angle. The deformation value D was calculated using Eq. (5).

$$D = \frac{P}{A} \times \frac{R_{eq}}{2} \quad (5)$$

Where P is the perimeter, and A is the projected surface area. R_{eq} is the equivalent radius, which is calculated by $A = \pi R_{eq}^2$.

2.2.1.11. Statistical analysis. In this study, IBM SPSS Statistics 22 (IBM SPSS Inc., USA) was used to perform One-way ANOVA with Tukey HSD.

Table 3
Formulations of the extrudate with/without emulsions, stabilised by potato protein (POPI-1 or POPI-2) or pea protein (PPI).

Sample name	Water	POPI-1 10 wt%	POPI-2 10 wt%	PPI 10 wt%	POPI-1 15 wt%	POPI-2 15 wt%	PPI 15 wt%
SPC (wt%)	43.3	43.3	43.3	43.3	43.6	43.6	43.6
Water or Emulsion (wt%)	56.7	56.7	56.7	56.7	56.4	56.4	56.4
pH of emulsion	–	7.0	3.6	7.0	7.0	3.6	7.0
Conductivity of emulsion (μS/cm)	–	1500	1500	1500	1500	1500	1500
Oil in extrudate from emulsion (wt%)	–	5.67	5.67	5.67	8.45	8.45	8.45

The significance was defined as $P < 0.05$, and significant differences were marked with different letters.

3. Results and discussion

3.1. Extrudate analysis

Six types of extrudates (Table 3) were produced using different emulsions (Table 2). Since the inclusion of oil can cause processing instabilities, the solid content was measured to check whether the extrusion was conducted without any problems. For all extrudates, including the control, made only from SPC and water, the solid content was determined by averaging the measurements in four extrudate pieces each from the two replicated extrusion experiments (n = 8 in total) (Fig. S2). The solid content differed only slightly within the samples with the same oil content and almost matched the calculated values based on feed composition. The extrudates containing oil in the form of emulsions had a slightly higher solid content than the value of those produced by just adding the oil to the control since there was also an amount of protein (and salt) in the emulsions added to the feed.

3.1.1. Surface oil and oil leakage

For all samples, their surface oil and rate of oil leakage from the cooling die of the extruder were measured and are shown in Fig. 1. For the extrudates prepared with 10 wt% oil emulsions, the extrudate prepared with the POPI-2-stabilised emulsion had a significantly larger amount of oil on the surface (Fig. 1A) than the extrudates in which the emulsion was prepared with POPI-1 and PPI. For the samples with 15 wt % oil, all extrudates had considerably more surface oil than at 10 wt%. PPI showed a significantly lower amount of oil on the surface of those extrudates compared to the samples prepared with POPI-1 and POPI-2 (Fig. 1A). When the oil content in the emulsions increased, the oil droplets had a higher chance to collide with each other and coalesce, and more of those coalesced larger droplets were expelled from the protein matrix. When the rate of oil leakage was measured, no oil drops leaked from the cooling die with 10 wt% oil (Fig. 1B). For the 15 wt% oil emulsions, all samples showed significant oil leakage from the die. PPI showed the lowest amount of oil leakage.

The observation that the extrudate with the PPI-stabilised emulsion had the lowest surface oil and lowest leakage rate is interesting. In small amplitude oscillatory surface shear and dilatational measurements, the PPI-stabilised interface had the lowest shear and dilatational storage moduli of the three stabilisers (Ikenaga and Sagis, 2024). POPI-2 had the highest modulus in dilatational deformations and appeared to perform worst here with respect to emulsion stabilisation during extrusion. In large amplitude oscillatory surface shear, the POPI-2 stabilised oil-water interface was shown to be more brittle (Ikenaga and Sagis, 2024), whereas POPI-1 formed similarly stiff but more stretchable interfaces (i.e. with a higher maximum linear strain). The PPI stabilised oil-water interface had the largest maximum linear strain in surface shear mode, and the transition to plastic behaviour was much more gradual than in the other two samples. It also showed only limited softening in large amplitude oscillatory dilatation. As a result of the higher brittleness, the shear forces in the extruder may have induced significantly more rupture of the oil-water interface in the extrudates with the POPI-1 and POPI-2 stabilised emulsion. For POPI-2, there may be an additional effect of a change in pH, from the original value of 3.6 to higher values, because of the high amount of added SPC in the extrudate mixture. POPI-2 was specifically developed for applications at acidic pH, and an increase in pH might have lowered the emulsion stability.

It appears that the high stiffness of the oil-water interface in the linear regime is not a good indicator of emulsion stability during extrusion. This stability appears to be controlled by the stretchability of the interface and the degree of softening in the nonlinear regime. As a result, the weaker PPI-stabilised interface performs better than the POPI-stabilised samples.

3.1.2. Blade cutting

The cutting force of the extrudates was measured in the transverse and longitudinal directions (Fig. 2). The extrudate prepared with POPI-1-stabilised emulsion had a significantly higher value in both F_t and F_l than the extrudates with the other two emulsions, at both oil contents. The presence of oil droplets can affect protein structuring (Kyriakopoulou, Keppler and van der Goot, 2021), and the observed difference could be caused by differences in the distribution of droplets, their size, and degree of deformation and orientation. We will address these parameters in Sec. 3.3.

3.1.3. Tensile experiments

To further characterise the protein structures, tensile experiments were performed by cutting the extrudate into a dog-bone shape (Fig. 3) (Pietsch et al., 2019). Compared to the control (prepared with just water, no oil added), the extrudates with 10 wt% oil emulsions showed similar Young's modulus, fracture strain, and fracture stress. POPI-1 (10 wt%) had a slightly higher Young's modulus, suggesting that POPI-1-stabilised emulsion caused a somewhat lower degree of disruption of the protein structure compared to the other two samples (Pietsch et al., 2019). This could again be linked to differences in droplet size and distribution. The samples with 15% oil all showed lower Young's modulus, lower fracture stress, and significantly lower fracture strain

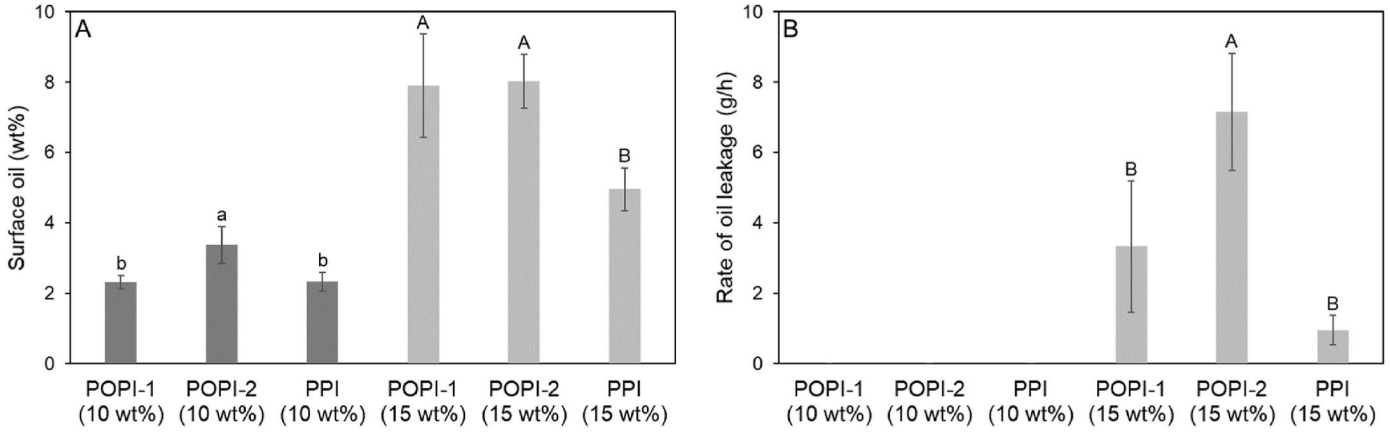

Fig. 1. Surface oil on the extrudates (A) and the rate of oil leakage from the cooling die (B). The measurement was performed on four extrudate pieces, each from the two replicated extrusion experiments, n = 8 in total for surface oil. The leaked oil was collected twice for approximately 10 min for each measurement, each on the two replicated extrusion experiments, n = 4 in total. Different letters indicate statistical differences for each different oil content group. Emulsions stabilised by potato protein (POPI-1 and POPI-2) or pea protein (PPI) were used to make the extrudates.

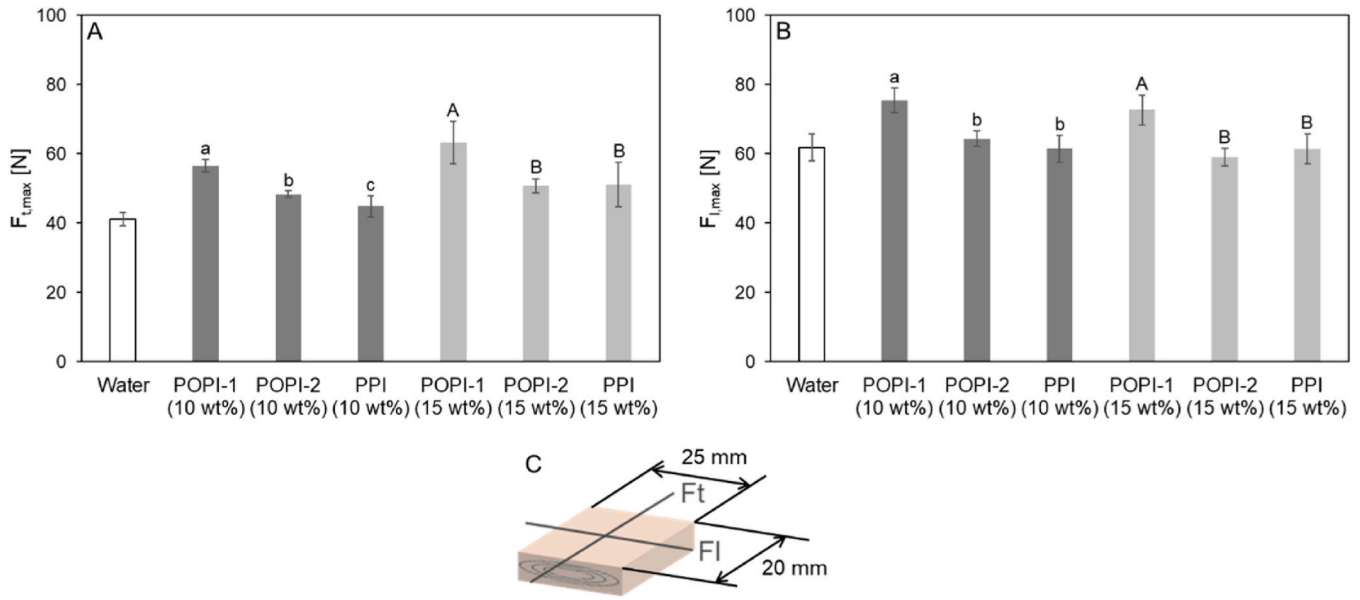

Fig. 2. $F_{t,max}$ (A) and $F_{l,max}$ (B) of the extrudates. The directions for F_t and F_l are indicated in (C). The measurement was performed on six extrudate pieces each from the two replicated extrusion experiments, n = 12 in total. Different letters indicate statistical differences for each different oil content group. Emulsions stabilised by potato protein (POPI-1 or POPI-2) or pea protein (PPI) were used to make the extrudates.

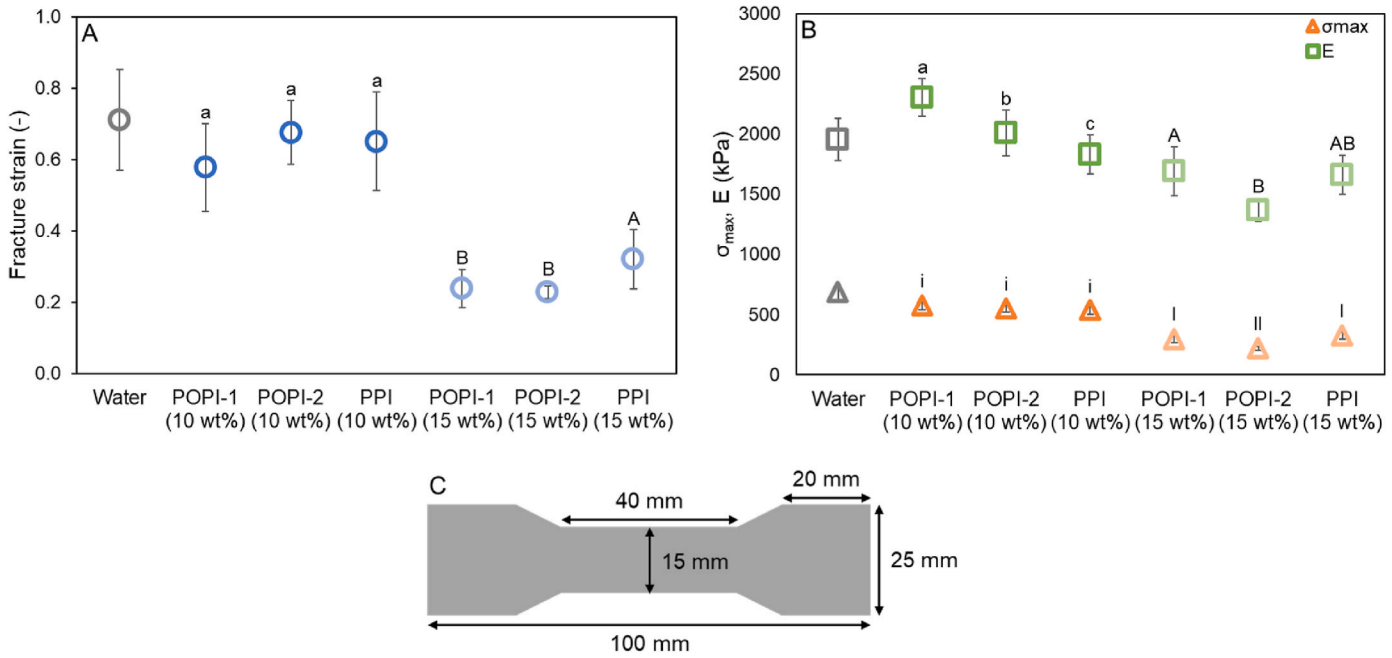

Fig. 3. Fracture strain (A), fracture stress (B), and Young's modulus (B) of the extrudates. The measurement was performed on six extrudate pieces each from the two replicated extrusion experiments, n = 12 in total. Different letters indicate statistical differences for each different oil content group. Emulsions stabilised by potato protein (POPI-1 or POPI-2) or pea protein (PPI) were used to make the extrudates.

than the samples with 10% oil, indicating that this level of oil content significantly affected the structure formation of the protein matrix. This was also observed by Gwiazda et al. (1987); Kendler et al. (2021), who suggested that high oil levels can significantly prevent formation of aligned fibrous structures. The values of the fracture stress for the 10% samples are all around ~500 kPa, and for those with 15% oil the value for the fracture stress is about 250 kPa. The latter values are close the values found for cooked bovine muscle meat when measured in the direction along the fibers, which tend to be in the range of 250–300 kPa (Purslow, 1985; Lepetit and Culioli, 1994).

3.1.4. *Wedge length and angle*

The wedge length and wedge angle were also measured, and the results are shown in Fig. 4. As can be seen from the images (Fig. 4C and D), all samples had a fibrous texture, regardless of oil content. For the wedge length, there were no significant differences between the three extrudates with 10 wt% oil emulsions, but all had a considerably lower wedge length than the extrudate without oil. Adding up to 15 wt% oil caused a further reduction of the wedge length, which is in line with the significant reduction in fracture strain for these samples in the tensile strength measurements (Fig. 3A). For these 15 wt% samples, PPI, the sample with the highest fracture strain, also had the longest wedge

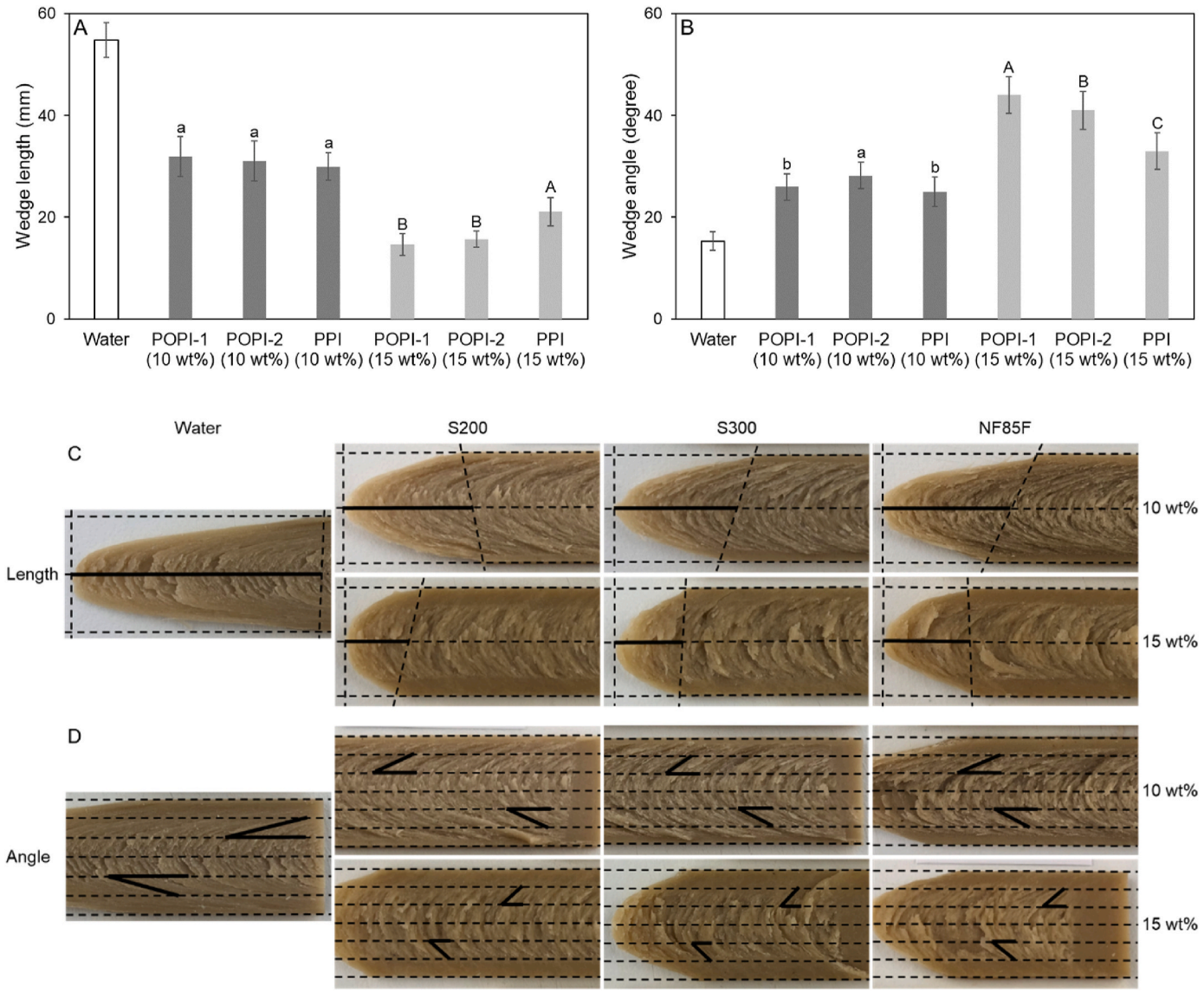

Fig. 4. Wedge length (A) and angle (B) of the extrudates and the analysed images. The measurements were performed on six different wedges on the extrudate, each from the two replicated extrusion experiments (n = 12 in total), and on six angle data, each on the 2nd and 5th slices, for two replicated extrusion experiments (n = 24 in total). Different letters indicate statistical differences for each different oil content group. Emulsions stabilised by potato protein (POPI-1 or POPI-2) or pea protein (PPI) were used to make the extrudates.

length. At the higher oil content, emulsion stability and interfacial properties seem to have a stronger influence on protein structuring. Similar reductions in the anisotropy of the protein structure were also observed by Kendler et al. (2021), upon increasing oil content by direct oil addition to the extrudate.

A longer wedge length correlates with a smaller wedge angle, with the oil-free sample having the smallest angle. Again, this difference in length and angle indicates that the oil droplets affect the protein structuring in different ways according to their size, number, and possibly also the nature of the stabiliser (i.e., interacting or non-interacting with the protein matrix). The shorter wedge length and larger angle, due to higher oil content, were previously also observed by Akdogan (1999), and there it was proposed that the higher oil content might decrease the dough's apparent viscosity, resulting in less structuring (Ilo et al., 2000).

3.1.5. *Multiphoton excitation microscopy*

To further study how oil droplets were distributed in the protein structures, all extrudates were observed in three FOVs using a multiphoton excitation microscope. As can be observed in the fluorescent images (Fig. 5), the proteins (magenta) were oriented and texturised by the extruder in the direction of flow. As discussed (Gwiazda et al., 1987; Kendler et al., 2021; Wang et al., 2022), with oils or emulsions, there were a lot of oil droplets in the water-filled pores, and the protein structures completely covered some of them. Compared to the previous study (Wang et al., 2022), in our samples, more large droplets were observed in the water pores between the protein structures. A possible reason for this could be the fact that multiphoton excitation microscopy allows for non-destructive observation to a substantial depth within the sample without the need for sectioning. Most droplets seemed to be sticking to the protein structures because they did not move during observation. However, some of them were moving in the water pockets. Free oil droplets might coalesce during storage, similar to what happens in the ageing of emulsions (Tang, 2017). Clearly, for all samples, a considerable number of droplets was larger than 10 μm. Since the main peak in the size distribution of the emulsions before the extrusion process was at 0.9–1.0 μm, coalescence has occurred during the extrusion process. Image analysis was used to determine whether there are significant differences between the three FOVs of the protein sources used

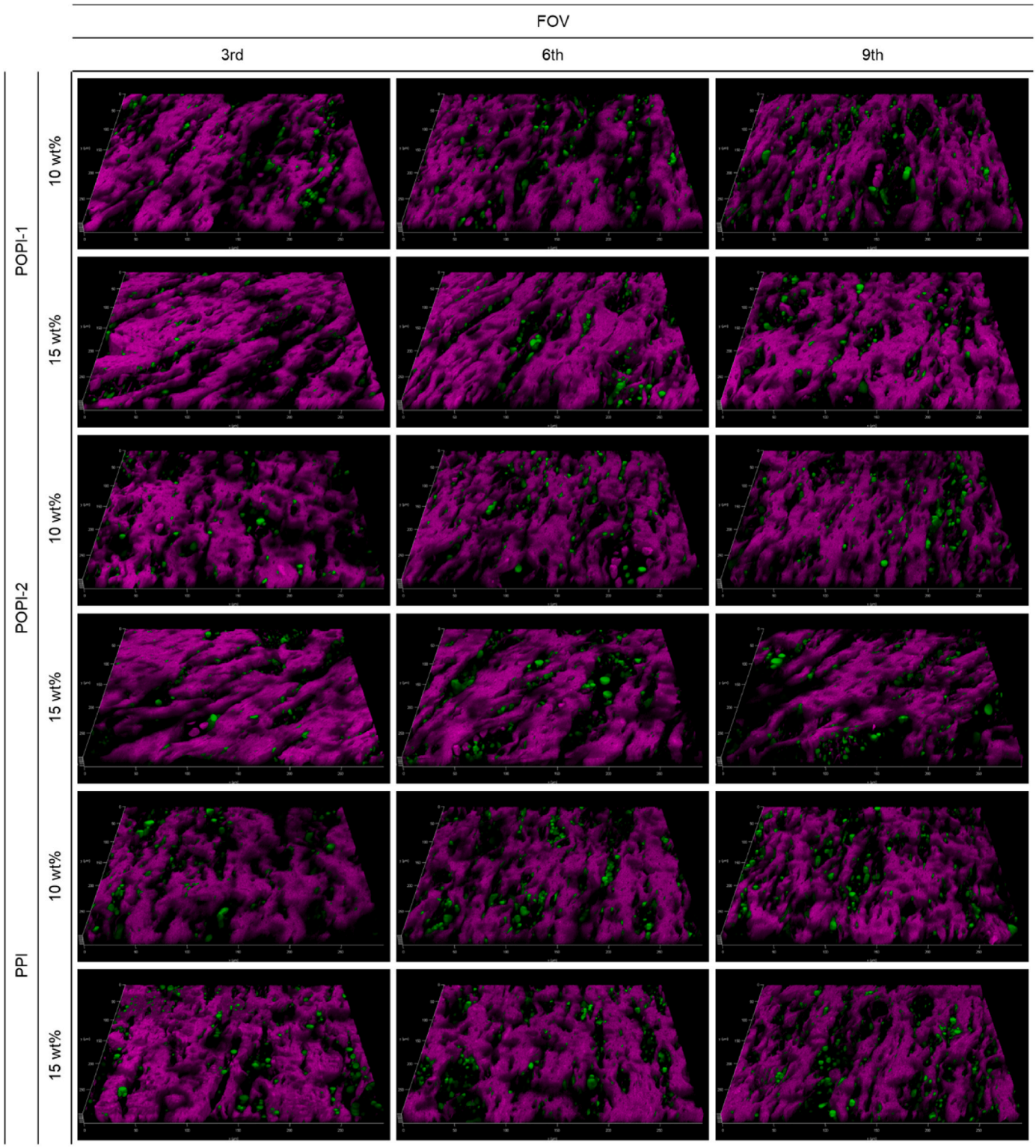

Fig. 5. Multiphoton microscopic images of the extrudates. The FOVs were the 3rd, 6th, and 9th slices (see Sec. 2.2.1.10) from left to right. The 3D image is a rectangle with a height of 10 μm, a width of 294 μm, and a depth of 294 μm (a tick is 50 μm). The protein structures and oil droplets are shown in magenta and green. For clarity, one representative result for each is shown, but comparable results were obtained for two replicates. Emulsions stabilised by potato protein (POPI-1 or POPI-2) or pea protein (PPI) were used to make the extrudates.

for stabilising the emulsions with respect to the structure of the extrudate. The results of this analysis are discussed in the next section.

3.2. Image analysis

To study how oil droplets deformed in the extrudate during the extrusion process, the multiphoton images of that were analysed using the image processing software ImageJ.

3.2.1. Degree of deformation

To determine the degree of the deformation, the perimeter and surface area of all droplets were determined with ImageJ, and the droplet deformation was calculated using equation (5). The obtained values were averaged and compared (Fig. 6). The perimeter increases when the shape of a droplet changes from a circle to a distorted shape with the same area. As the results of the image analysis show, PPI gave a significantly higher value in each FOV with 15 wt% oil (Fig. 6C), while for the 10 wt% oil samples, only the 9th FOV had significantly more deformed droplets than the POPI samples. It is likely that PPI's softer interface was more deformed by the shear and protein structuring. Regarding the comparison between the FOVs (Fig. 6B and D), all the extrudates except for POPI-2 showed a significant increase in deformation of the oil droplets from the 3rd to the 9th FOV. For POPI-2, the droplets were less deformed only at the 3rd FOV. This might be caused by the higher surface oil and oil leakage in that sample. The larger droplets could have been expelled from the extrudate, and the droplets left behind were smaller and less affected by the shear and protein structuring. These remaining oil droplets could have affected the structure, by binding to the matrix by protein-protein interactions (e.g., hydrogen bonding, hydrophobic interactions), and locally stiffening the matrix. From that point of view, it is possible to explain why the hardness of the POPI-1 extrudate was the highest in the blade cutting test (Fig. 2A and B). This again shows that to understand the deformation of the oil droplets in the extrusion process, it is essential to consider the protein structuring and the oil expelled from the extrudate, which are linked to the characteristics of the droplet's interface (see Fig. 7).

3.2.2. Degree of droplet orientation

In addition to the shape of the droplets, their orientation is an important parameter, and the degree of droplet orientation was calculated from the standard deviation (SD) of the average orientation angle of all deformed droplets. The oil droplet orientation in the 3rd FOV was significantly more scattered than the other two FOVs for all extrudates at 10 wt% and all stabilisers. However, there was almost no difference when comparing the stabilisers at the same FOV, at 10 wt% oil. This again suggests that the deformation of the oil droplets in these samples was mostly dominated by the protein structuring and flow, and, to a lesser extent, by the interfacial properties of the oil droplets.

The extrudates at 15 wt% oil had the same trend: the droplets were less oriented in the flow direction at the 3rd FOV. However, POPI-2 (15 wt%) had a significantly lower SD value than the other two extrudates at the 3rd FOV. The higher values of the SD at the 3rd FOV were thought to mean the droplets were fixed by the protein structuring caused by a quick cooling near the cooling die.

4. Conclusions

This study investigated how emulsion stability and interfacial properties affect protein structuring and oil droplet deformation during the extrusion of HMMAs. When emulsions with 10 wt% or 15 wt% oil were included in the HMMA extrusion, the appearance of the extrudates and their physical properties were clearly affected. At 15 wt% oil, PPI gave significantly less surface oil and a much lower rate of oil leakage than the other two samples, whereas POPI-2 had the highest oil leakage. It appears that, particularly at higher oil content, the softness and stretchability of the emulsion interface stabilised by PPI gives better oil retention in the extrudate than a stabiliser that produces stiff and brittle interfaces.

When focusing on the structure, the blade-cutting experiments

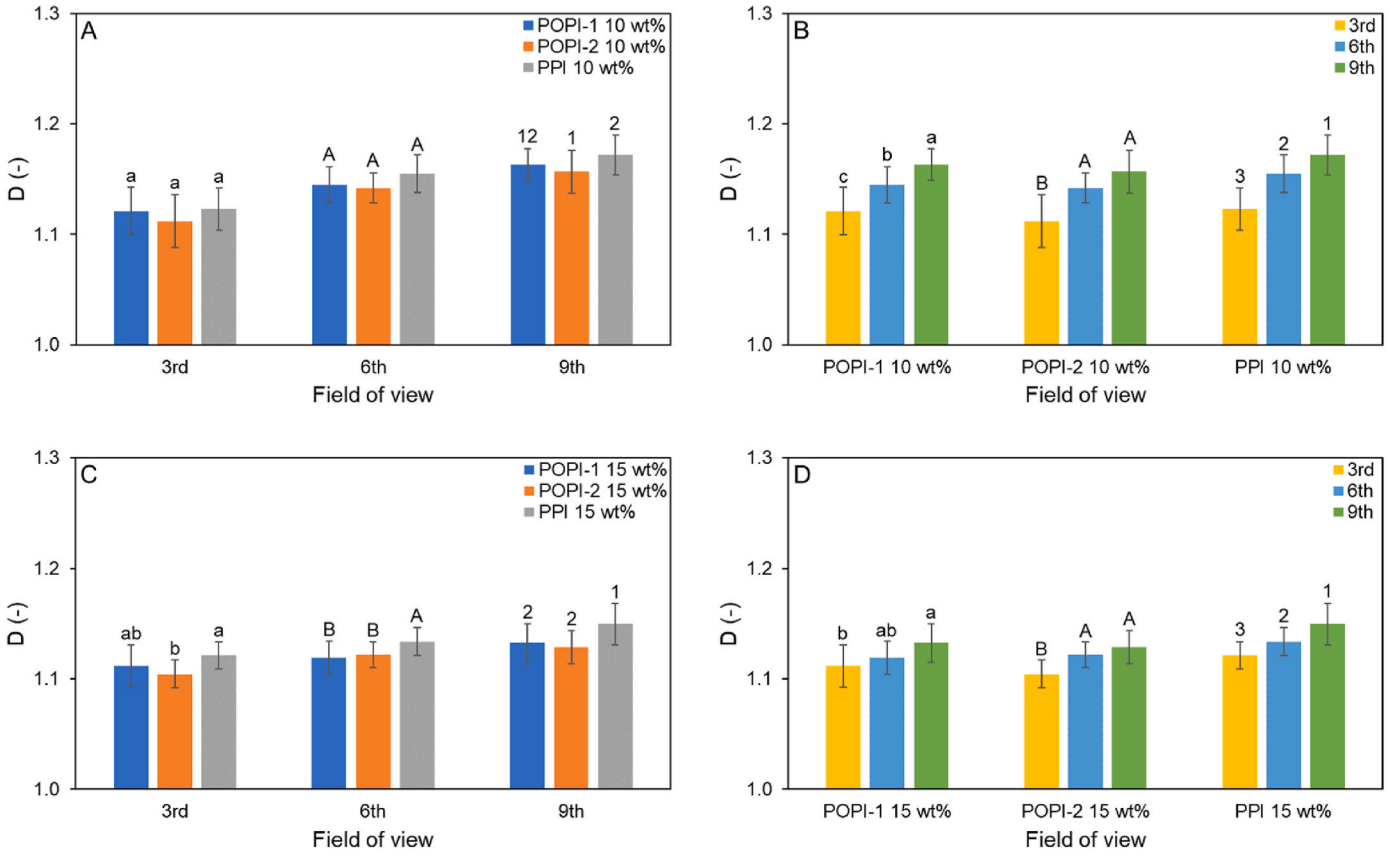

Fig. 6. The degree of the oil droplet deformation compared based on the average D values calculated with Eq. (5) in different FOVs. Nine images were used from at least three cross-sections (Max. is three images for one cross-section) for each of the two replicates, n = 18 in total. Different letters indicate statistical differences for each comparison. Emulsions stabilised by potato protein (POPI-1 or POPI-2) or pea protein (PPI) were used to make the extrudates.

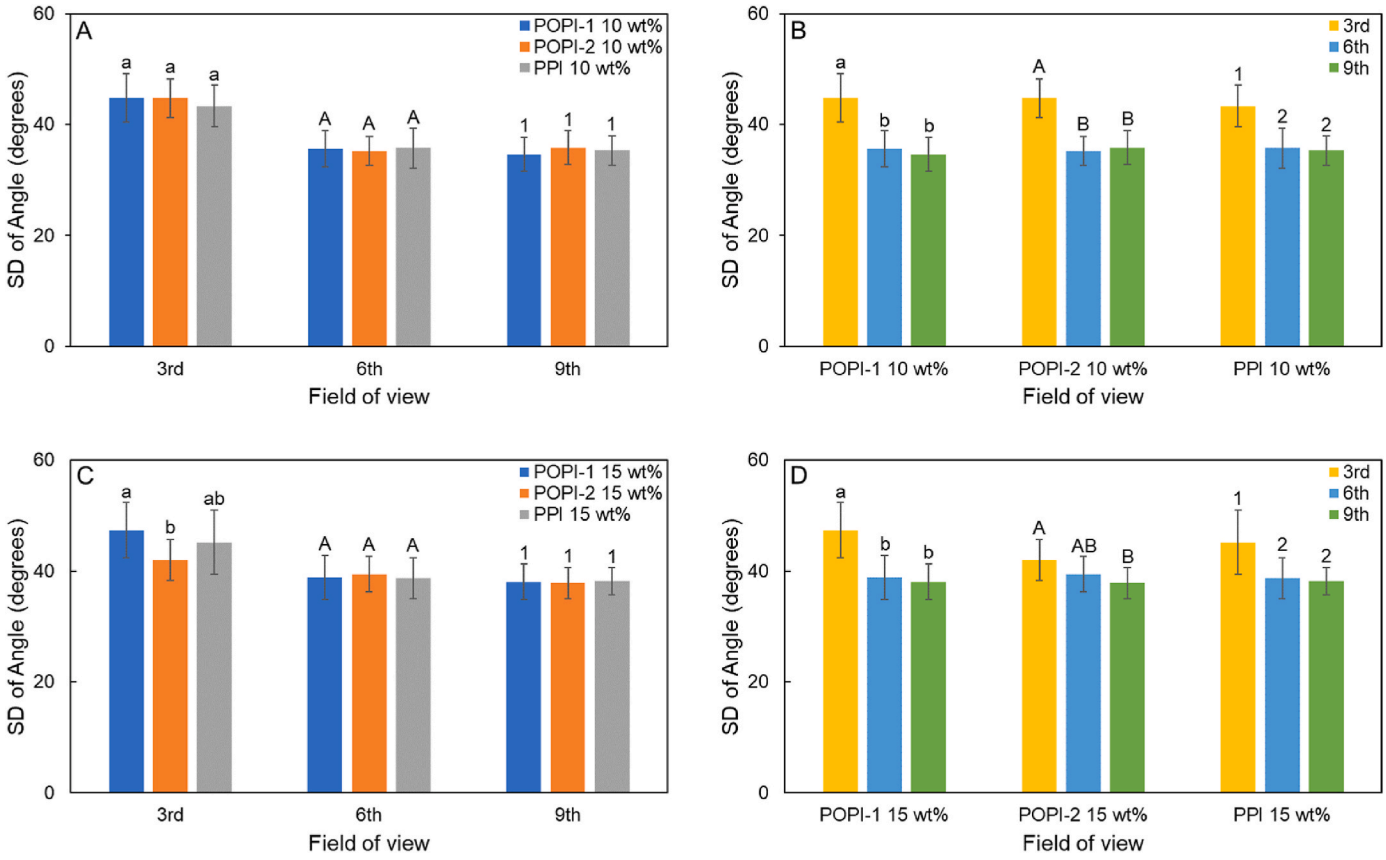

Fig. 7. The degree of the oil droplet orientation compared in terms of the standard deviation of the angle. Nine images were used from at least three cross-sections for each of the two replicates, n = 18 in total. Different letters indicate statistical differences for each comparison. Emulsions stabilised by potato protein (POPI-1 or POPI-2) or pea protein (PPI) were used to make the extrudates.

showed the highest value for the cutting force in the extrudates with POPI-1 (10 wt% and 15 wt%). In the tensile experiments, at 10 wt% oil, POPI-1 also had the highest Young's modulus, and PPI had the lowest modulus. At 15 wt% oil, POPI-1 and PPI gave similar moduli and were stiffer than POPI-2. PPI had the longest wedge length at 15 wt% oil, and POPI-1 and -2 were similar in that aspect. PPI also gave the highest value for the fracture strain. The higher oil loss clearly affected the structure and strength of the POPI-2 sample.

Multiphoton microscopy showed that some degree of coalescence had occurred during the extrusion process, but there was still a significant fraction of droplets of a small size. This was also observed when the emulsions were subjected to high shear using an Ultra Turrax (Ikenaga and Sagis, 2024). The image analyses showed that oil droplets near the extrudate surface were less deformed and less oriented than in the centre parts in the extrudates with 10% oil. It is likely that the protein structure and, thereby, the shape and orientation of the droplets were fixed near the surface much sooner than the protein structure at the centre. Increasing the oil fraction from 10 wt% to 15 wt% made this difference smaller, suggesting that protein structuring was more disrupted throughout the sample by the larger amount of oil. This is also confirmed by the fact that at 15 wt% oil, all samples have shorter wedge length, lower Young's modulus, lower fracture strain and lower fracture stress.

The results of this study suggest that a softer and more stretchable oil-water interface is more favourable to incorporate significant amounts of oil in an HMMA product during the extrusion process. These results can be useful for the development of new HMMAs in which oil is included in the form of an emulsion, and, in particular, can help with the choice of emulsifier for the stabilisation of the emulsion.

CRediT authorship contribution statement

Naoya Ikenaga: Writing – original draft, Validation, Investigation, Formal analysis. **Shuzo Hashimoto:** Writing – review & editing, Validation, Investigation. **Leonard M.C. Sagis:** Writing – review & editing, Supervision, Project administration, Methodology, Conceptualization.

Declaration of competing interest

The authors declare that no competing interests exist.

Acknowledgement

This research is part of the project PlantPROMISE, which is co-financed by Top Consortium for Knowledge and Innovation Agri & Food by the Dutch Ministry of Economic Affairs; The project is registered under contract number LWV-19027.

Appendix A. Supplementary data

Supplementary data to this article can be found online at https://doi.org/10.1016/j.jfoodeng.2024.112353.

Data availability

Data will be made available on request.

References

Akdogan, H., 1999. High moisture food extrusion. Int. J. Food Sci. Technol. 34 (3), 195–207.

Akharume, F.U., Aluko, R.E., Adedeji, A.A., 2021. Modification of plant proteins for improved functionality: a review. Compr. Rev. Food Sci. Food Saf. 20 (1), 198–224.
Choi, Y.M., Garcia, L.G., Lee, K., 2019. Correlations of sensory quality characteristics with intramuscular fat content and bundle characteristics in bovine longissimus thoracis muscle. Food science of animal resources 39 (2), 197.
Cornet, S.H., Snel, S.J., Schreuders, F.K., van der Sman, R.G., Beyrer, M., van der Goot, A. J., 2022. Thermo-mechanical processing of plant proteins using shear cell and high-moisture extrusion cooking. Crit. Rev. Food Sci. Nutr. 62 (12), 3264–3280.
Emin, M., Schuchmann, H., 2013. Droplet breakup and coalescence in a twin-screw extrusion processing of starch based matrix. J. Food Eng. 116 (1), 118–129.
Guo, Z., Teng, F., Huang, Z., Lv, B., Lv, X., Babich, O., Yu, W., Li, Y., Wang, Z., Jiang, L., 2020. Effects of material characteristics on the structural characteristics and flavor substances retention of meat analogs. Food Hydrocolloids 105, 105752.
Gwiazda, S., Noguchi, A., Saio, K., 1987. Microstructural studies of texturized vegetable protein products: effects of oil addition and transformation of raw materials in various sections of a twin screw extruder. Food Struct. 6 (1), 8.
Ikenaga, N., Sagis, L.M., 2024. Interfacial moduli at large strains and stability of emulsions stabilised by plant proteins at high bulk shear rates. Food Hydrocolloids 146, 109248.
Ilo, S., Schoenlechner, R., Berghofe, E., 2000. Role of lipids in the extrusion cooking processes. Grasas Aceites 51 (1–2), 97–110.
Kendler, C., Duchardt, A., Karbstein, H.P., Emin, M.A., 2021. Effect of oil content and oil addition point on the extrusion processing of wheat gluten-based meat analogues. Foods 10 (4), 697.
Köllmann, N., Schreuders, F.K., Zhang, L., van der Goot, A.J., 2023. On the importance of cooling in structuring processes for meat analogues. J. Food Eng. 350, 111490.
Kyriakopoulou, K., Keppler, J.K., van der Goot, A.J., 2021. Functionality of ingredients and additives in plant-based meat analogues. Foods 10 (3), 600.
Lepetit, L., Culioli, J., 1994. Mechanical properties of meat. Meat Sci. 36, 203–237.
Mäkinen, O.E., Wanhalinna, V., Zannini, E., Arendt, E.K., 2016. Foods for special dietary needs: non-dairy plant-based milk substitutes and fermented dairy-type products. Crit. Rev. Food Sci. Nutr. 56 (3), 339–349.
Mefleh, M., Pasqualone, A., Caponio, F., Faccia, M., 2022. Legumes as basic ingredients in the production of dairy-free cheese alternatives: a review. J. Sci. Food Agric. 102 (1), 8–18.
Munekata, P.E., Domínguez, R., Budaraju, S., Roselló-Soto, E., Barba, F.J., Mallikarjunan, K., Roohinejad, S., Lorenzo, J.M., 2020. Effect of innovative food processing technologies on the physicochemical and nutritional properties and quality of non-dairy plant-based beverages. Foods 9 (3), 288.
Nieuwland, M., Heijnis, W., van der Goot, A.-J., Hamoen, R., 2023. XRT for visualizing microstructure of extruded meat replacers. Curr. Res. Food Sci. 6, 100457.
Osen, R., Toelstede, S., Wild, F., Eisner, P., Schweiggert-Weisz, U., 2014. High moisture extrusion cooking of pea protein isolates: raw material characteristics, extruder responses, and texture properties. J. Food Eng. 127, 67–74.
Pietsch, V.L., Emin, M.A., Schuchmann, H.P., 2017. Process conditions influencing wheat gluten polymerization during high moisture extrusion of meat analog products. J. Food Eng. 198, 28–35.
Pietsch, V.L., Werner, R., Karbstein, H.P., Emin, M.A., 2019. High moisture extrusion of wheat gluten: relationship between process parameters, protein polymerization, and final product characteristics. J. Food Eng. 259, 3–11.
Purslow, P.P., 1985. The physical basis of meat texture: observations on the fracture behaviour of cooked bovine M. Semitendinosus. Meat Sci. 12, 39–60.
Sagis, L.M., Yang, J., 2022. Protein-stabilized interfaces in multiphase food: comparing structure-function relations of plant-based and animal-based proteins. Curr. Opin. Food Sci. 43, 53–60.
Singh, M., Trivedi, N., Enamala, M.K., Kuppam, C., Parikh, P., Nikolova, M.P., Chavali, M., 2021. Plant-based meat analogue (PBMA) as a sustainable food: a concise review. Eur. Food Res. Technol. 247 (10), 2499–2526.
Tang, C.-H., 2017. Emulsifying properties of soy proteins: a critical review with emphasis on the role of conformational flexibility. Crit. Rev. Food Sci. Nutr. 57 (12), 2636–2679.
Wang, H., Zhang, L., Czaja, T.P., Bakalis, S., Zhang, W., Lametsch, R., 2022. Structural characteristics of high-moisture extrudates with oil-in-water emulsions. Food Res. Int. 158, 111554.
Zhang, J., Liu, L., Jiang, Y., Faisal, S., Wang, Q., 2020. A new insight into the high-moisture extrusion process of peanut protein: from the aspect of the orders and amount of energy input. J. Food Eng. 264, 109668.